

CHAPTER III

SIMPLE POTENTIAL SCATTERING

III.1. Introduction

The semiclassical method discussed in the previous chapter has already been applied to some problems involving real potentials^{1,2}. The method has remarkable simplicity and a fair degree of accuracy and, therefore, appears to be a suitable candidate for adaptation for a complex potential. To study the efficacy of the method for a complex potential, we have considered in this chapter three simple examples:

(A) The first example³ involves a potential consisting of a repulsive coulomb term and an imaginary term of the form $i\beta/r^2$. The Schrödinger radial equation with this potential can be solved exactly and the phase shifts can be obtained analytically. The semiclassical phase shifts, obtained by complex Miller-Good method, (CMG) have been shown to agree very well with the exact phase shifts. We have also studied the variations of the phase shifts with β , which gives the strength of the absorptive part. Although the heavy ion potential is much more complicated than this potential, both share the common feature of a short range absorptive part and a long range coulomb tail. To check the accuracy of the CMG method we have also considered two other⁴ simple examples:

(B) Exponential: $V = -V_0 e^{-\gamma r}$ and (C) Yukawa: $V = -\frac{V_0}{r} e^{-\gamma r}$.

The semiclassical phase shifts calculated for real potentials of type (B) and (C) have been compared with their exact values (obtained numerically) and also with some other results obtained by different approximation methods. The semiclassical method gives fairly accurate phase shifts, even at lower energies, say for $K \sim 1 \text{ fm}^{-1}$. The potentials were then made complex by making V_0 complex, and the CMG phase shifts were computed. For the sake of completeness, we have also presented a treatment of the complex potential, in which the imaginary part of the potential is treated as a perturbation and only terms of the first order are considered. The method, as expected, is accurate only for a small absorption.

III.2. An exactly solvable model

We shall consider here the scattering from a potential $a/r - i\beta/r^2$. The presentation of the results will be as follows. In the sec. III.2.1, the problem has been studied exactly. The section III.2.2 gives the semiclassical treatment for the same problem, while the section III.2.3 gives the perturbative treatment. In section III.2.4, the semiclassical as well as perturbative results have been presented and compared with the exact results.

III.2.1. Exact complex phase shifts

The radial Schrödinger equation with a potential $V(r) = a/r - i\beta/r^2$ is given by

$$\frac{1}{r^2} \frac{d}{dr} \left[r^2 \frac{dR_L}{dr} \right] + \left[K^2 - \frac{2nK}{r} - \frac{L(L+1) - i\beta}{r^2} \right] \times R_L(r) = 0, \quad \dots(3.1)$$

where

$$n = \frac{\mu ZZ' e^2}{\hbar^2 K}, \quad K = (2 \mu E / \hbar^2)^{1/2}.$$

Let $\ell = p + iq$, $p > 0$, be a solution of the equation

$$\ell(\ell + 1) = L(L + 1) - i\beta. \quad \dots(3.2)$$

Let us make the substitution

$$R_L(r) = r^\ell e^{iKr} f_\ell(r)$$

in Eq. (3.1), which gives

$$r f_\ell''(r) + (2iKr + 2\ell + 2) f_\ell'(r) + [2iK(\ell + 1) - 2nK] \times f_\ell(r) = 0. \quad \dots(3.3)$$

The solution of this equation can be written as

$$f_\ell(r) = C_\ell {}_1F_1(\ell + 1 + in, 2\ell + 2, -2iKr), \quad \dots(3.4)$$

where C_ℓ is the normalization constant. We will have to impose the appropriate boundary condition on (3.4). In particular, one has to ensure that there is no attenuation of the incoming wave. The asymptotic form of $R_\ell(r)$ is then given by

$$R_\ell(r) \rightarrow C_\ell \frac{\Gamma(2\ell + 2)}{(2K)^\ell Kr} \frac{e^{n\pi/2} e^{q\pi/2}}{\Gamma(p + 1 + iq - in)} \frac{1}{2i} \times \left[e^{is} - (A + iB)e^{-is} \right], \quad \dots(3.5)$$

where

$$A + iB = \frac{\Gamma(p + 1 + iq - in)}{\Gamma(p + 1 + iq + in)} e^{-q\pi}, \quad \dots(3.6)$$

and

$$s = Kr - \frac{1}{2} p\pi - n \ln 2Kr. \quad \dots(3.7)$$

The case of a real coulomb potential is well known. The corresponding solution has the asymptotic behaviour

$$R_L(r) \rightarrow C_\ell \frac{e^{n\pi/2 + i\sigma_L^c} \Gamma(2L + 2)}{(2K)^L Kr \Gamma(L + 1 + in)} \times \sin \left(Kr - \frac{L\pi}{2} - n \ln 2Kr + \sigma_L^c \right), \quad \dots(3.8)$$

where

$$\sigma_L^c = \arg \Gamma(L + 1 + in). \quad \dots(3.9)$$

Since the imaginary part of the potential vanishes for large r , it should be possible to rewrite the Eq. (3.5) in the form (3.8) with the inclusion of an additional phase shift. We, therefore, define the complex phase shifts $\eta_L = \mu + i\lambda$ through the relation

$$\sin \left(Kr - \frac{L\pi}{2} - n \ln 2Kr + \mu + i\lambda \right) = \frac{1}{2i} \left[e^{is} - (A+iB)e^{-is} \right]. \quad \dots(3.10)$$

The complex phase shifts η_L are then given by

$$\eta_L = (L - p) \frac{\pi}{2} - \frac{1}{2} \tan^{-1} (B/A) + \frac{i}{2} \ln (A^2 + B^2)^{\frac{1}{2}}. \quad \dots(3.11)$$

The phase shifts η_L have been determined for $n = 0.5, 2.0$ and 10.0 and different values of L and β and have been given in Tables I - III.

III.2.2. The semiclassical method

The Schrödinger radial equation for the problem can be written in the form

$$\frac{d^2 \Psi_\ell(y)}{dy^2} + \frac{t_1(y)}{\hbar^2} \Psi_\ell(y) = 0, \quad \dots(3.12)$$

where $y = Kr,$... (3.13)

and

$$t_1(y) = \hbar^2 \left[1 - \frac{2n}{y} - \frac{l(l+1) - 1\beta}{y^2} \right]. \quad \dots(3.14)$$

As the model equation, we choose, at the first instance, the radial equation for scattering from a point charge, with the same Sommerfeld parameter n . The model equation can be written as

$$\frac{d^2 \phi_l(s)}{ds^2} + \frac{t_2(s)}{\hbar^2} \phi_l(s) = 0, \quad \dots(3.15)$$

where

$$t_2(s) = \hbar^2 \left[1 - \frac{2n}{s} - \frac{l(l+1)}{s^2} \right]. \quad \dots(3.16)$$

The wave functions have the asymptotic forms

$$\Psi_l(y) \xrightarrow[\substack{\text{Lim} \\ y \rightarrow \infty}]{} \sin \left(y - \frac{l\pi}{2} - n \ln 2y + \sigma_{\text{complex}} \right), \quad \dots(3.17)$$

$$\phi_l(s) \xrightarrow[\substack{\text{Lim} \\ s \rightarrow \infty}]{} \sin \left(s - \frac{l\pi}{2} - n \ln 2s + \sigma_c \right). \quad \dots(3.18)$$

Regarding s as a function of y , and using the relation (2.20), we have,

$$\sigma_{\text{Complex}} - \sigma_c = \lim_{\substack{y \rightarrow \infty \\ s \rightarrow \infty}} \left(s - y - n \ln \frac{s}{y} \right). \quad \dots(3.19)$$

We shall use Langer's substitution and the superscript L will indicate that the function t_1 have been Langer substituted. There are two complex roots of the equation

$$t_1^L(y) = 0$$

in the present problem. One of these, however, does not qualify as a turning point because it has a negative real part. Let y_t denote the complex turning point for the present problem. The turning point, the trajectory, and the phase shifts are all real for the model equation. It is nevertheless possible to obtain the transformation (2.3). The complex phase shifts in the Zeroth order is given by

$$\begin{aligned} \sigma^0_{\text{Complex}} &= \sigma^C_L + \lim_{\substack{y \rightarrow \infty \\ S \rightarrow \infty}} (s - y - n \ln \frac{s}{y}) \\ &\approx \sigma^C_L + \int_{y_t}^{\tilde{y}} \left[y^2 - 2ny - (L + \frac{1}{2})^2 + i\beta \right]^{\frac{1}{2}} \frac{dy}{y} \\ &\quad - \left[\tilde{y}^2 - 2n\tilde{y} - (L + \frac{1}{2})^2 \right]^{\frac{1}{2}} + n \ln \left\{ \tilde{y} - n + \left[\tilde{y}^2 - 2n\tilde{y} - (L + \frac{1}{2})^2 \right]^{\frac{1}{2}} \right\} \\ &\quad - \frac{1}{2} n \ln \left[n^2 + (L + \frac{1}{2})^2 \right] - (L + \frac{1}{2}) \left[\sin^{-1} \left[\frac{n\tilde{y} + (L + \frac{1}{2})^2}{\tilde{y} \left[n^2 + (L + \frac{1}{2})^2 \right]^{\frac{1}{2}}} \right] - \frac{\pi}{2} \right] \\ &\quad + \frac{i\beta}{2(L + \frac{1}{2})} \left[\sin^{-1} \left[\frac{n\tilde{y} + (L + \frac{1}{2})^2}{\tilde{y} \left[n^2 + (L + \frac{1}{2})^2 \right]^{\frac{1}{2}}} \right] \right. \\ &\quad \left. - \sin^{-1} \left[\frac{n}{\left[n^2 + (L + \frac{1}{2})^2 \right]^{\frac{1}{2}}} \right] \right] \end{aligned} \quad \dots(3.20)$$

with σ_L^C given by (3.9). The second term on the right hand side is obtained by a complex integration. The integration contour has been shown in Fig. 2.1 in chapter II. The first order correction term Δ_L is given by

$$\Delta_L = -\frac{1}{12} \int_{S_t}^{\infty} \mathcal{L}[T_2(s)] [t_2^L(s)]^{\frac{1}{2}} ds \\ + \frac{1}{12} \int_{\mathcal{J}_t}^{\infty} \mathcal{L}[T_1(y)] [t_1^L(y)]^{\frac{1}{2}} dy, \quad \dots(3.21)$$

where $\mathcal{L}[T_i]$ is given by (2.14) and

$$T_1 = y^2 t_1^L(y), \quad T_2 = s^2 t_2^L(s). \quad \dots(3.22)$$

The expression for (3.21) can be simplified to

$$\Delta_L = -\frac{n}{24 \left[n^2 + \left(L + \frac{1}{2} \right)^2 \right]} \\ + \frac{n}{8} \int_{\mathcal{J}_t}^{\infty} \frac{[t_1^L(y)]^{\frac{1}{2}}}{(y-n)^4} y dy \quad \dots(3.23)$$

and is easily evaluated along the original contour. In Eq. (3.22), $t_1^L(y)$ and $t_2^L(s)$ are given by

$$t_1^L(y) = 1 - \frac{2n}{y} - \frac{(L + \frac{1}{2})^2 - i\beta}{y^2}$$

and

$$t_2^L(s) = 1 - \frac{2n}{s} - \frac{(L + \frac{1}{2})^2}{s^2} \dots(3.24)$$

The semiclassical phase shifts are then obtained as

$$\sigma_L = \sigma_{\text{Complex}}^0 + \Delta L \dots(3.25)$$

It is instructive to repeat the calculations with another model equation, which is given by the radial equation for a field free particle, viz.,

$$\frac{d^2 \phi(s)}{ds^2} + \frac{t_2(s)}{\hbar^2} \phi(s) = 0 \dots(3.26)$$

with

$$t_2(s) = 1 - \frac{L(L+1)}{s^2} \dots(3.27)$$

The phase shifts in this case are given by

$$\begin{aligned}
\sigma'_L &= \lim_{\substack{y \rightarrow \infty \\ s \rightarrow \infty}} (s - y + n \ln 2y) \\
&= \int_{y_t}^{y_t} \left[y^2 - 2ny - \left(L + \frac{1}{2}\right)^2 + i\beta \right]^{\frac{1}{2}} \frac{dy}{y} - n \\
&\quad - \left[\tilde{y}^2 - 2n\tilde{y} - \left(L + \frac{1}{2}\right)^2 \right]^{\frac{1}{2}} + \\
&\quad n \ln \left\{ \tilde{y} - n + \left[\tilde{y}^2 - 2n\tilde{y} - \left(L + \frac{1}{2}\right)^2 \right]^{\frac{1}{2}} \right\} - \\
&\quad \left(L + \frac{1}{2}\right) \left[\sin^{-1} \left[\frac{n\tilde{y} + \left(L + \frac{1}{2}\right)^2}{\tilde{y} \left[n^2 + \left(L + \frac{1}{2}\right)^2 \right]^{\frac{1}{2}}} \right] \right. \\
&\quad \left. - \sin^{-1} \left[\frac{n}{\left[n^2 + \left(L + \frac{1}{2}\right)^2 \right]^{\frac{1}{2}}} \right] - \frac{\pi}{2} \right] \\
&\quad + \frac{i\beta}{2 \left(L + \frac{1}{2}\right)} \left[\sin^{-1} \left[\frac{n\tilde{y} + \left(L + \frac{1}{2}\right)^2}{\tilde{y} \left[n^2 + \left(L + \frac{1}{2}\right)^2 \right]^{\frac{1}{2}}} \right] \right. \\
&\quad \left. - \sin^{-1} \left[\frac{n}{\left[n^2 + \left(L + \frac{1}{2}\right)^2 \right]^{\frac{1}{2}}} \right] \right] + \Delta'_L, \\
&\quad \dots(3.28)
\end{aligned}$$

where Δ'_L , the first order correction term, is given by

$$\Delta'_L = \frac{n}{8} \int_{y_t}^{\infty} \frac{[t_1^L(y)]^{\frac{1}{2}}}{(y-n)^4} \eta dy \quad \dots(3.29)$$

and $t_1^L(y)$ is given by the Eq. (3.24). The integrations in (3.28) and (3.29) are to be performed along the contour mentioned earlier.

III.2.3. Perturbative treatment

It may be interesting to note at this stage the results that one obtains by the perturbative treatment of the complex potential by the semiclassical method. The real part of the phase shift is obtained by a straightforward application of the JWKB method to the problem under consideration with the real part of the potential only. The real part of the phase shift is given by

$$\text{Re } \eta'_L = \left(L + \frac{1}{2}\right) \frac{\pi}{2} - Kr_0 + \int_{r_0}^{\infty} [K(r) - K] dr,$$

$$K(r) = K \left[1 - \frac{\left(L + \frac{1}{2}\right)^2}{K^2 r^2} - \frac{V(r)}{E} \right],$$

$$K(r_0) = 0, \quad \dots (3.30)$$

where r_0 is the classical turning point. Obviously, these results cannot be reliable since the real part of the phase shift given by (3.30) is seen to be independent

of β , whereas the exact phase shifts show a fairly good variation as β changes (Tables I - III and Fig. 3.1).

The imaginary part of the phase shift in first order in β is given by

$$I_m \eta_L = \frac{\beta}{2} \int_{r_0}^{\infty} \frac{dy}{y^2 \left[1 - \frac{(L + \frac{1}{2})^2}{y^2} - \frac{2n}{y} \right]^{\frac{1}{2}}} \dots (3.31)$$

The perturbative imaginary phase shifts are compared with exact and semiclassical results for $n = 0.5$ and different values of L and β and are shown in Fig.3.2.

III.2.4. Results and discussions

The CMG phase shifts calculated for $n = 0.5$, 2.0, 10.0 and various β for the two model equations are given in Tables I, II and III. It may be pointed out that both the real and the imaginary parts of the phase shifts agree fairly well with the exact results. The results for $L = 1$ are, however, much better than for $L = 0$. The accuracy improves with higher L . We can draw the following conclusions:

(a) The real part of the phase shift show a significant dependence on the imaginary part of the potential. For $L = 1$ the real part even changes sign as the

Fig. 3.1. The variation of the real and imaginary parts of the phase shifts with β for various values of L .

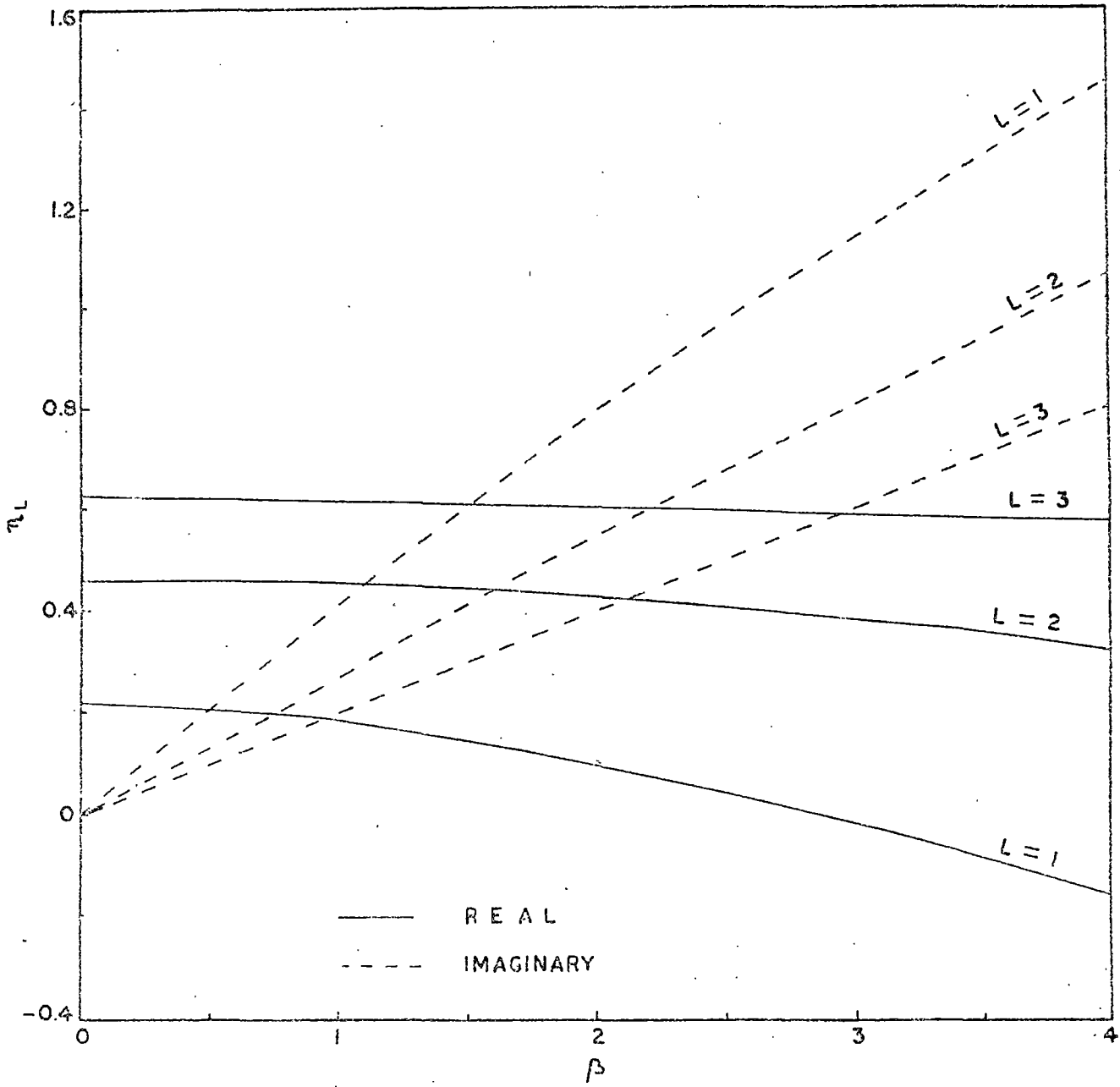


FIG. 3.1.

Fig. 3.2. Imaginary part of the phase shifts obtained by exact numerical, semi-classical and perturbative methods for $L = 0$ and 1.

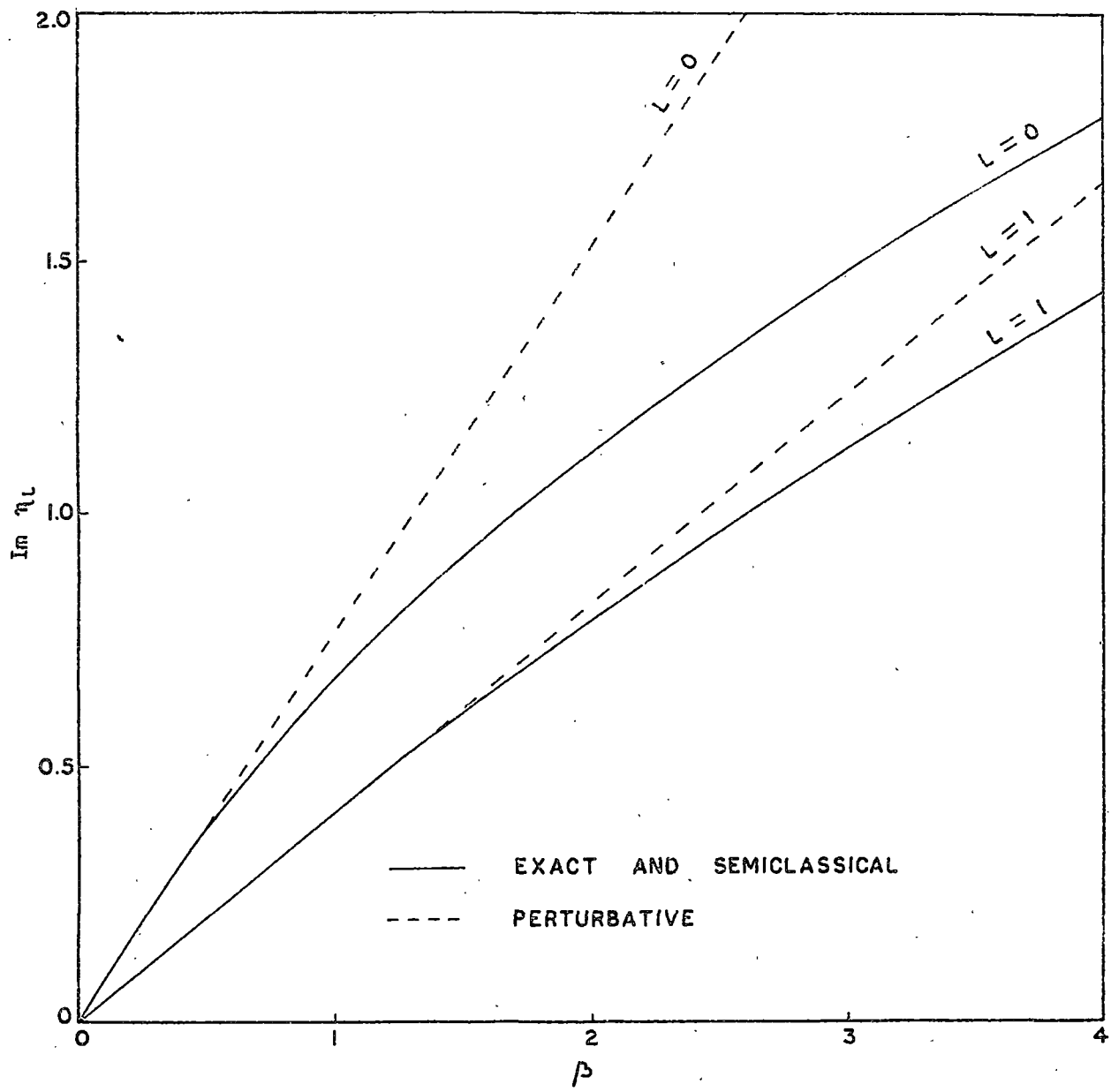


FIG. 3.2 .

TABLE I. The exact and the semiclassical phase shifts
for $n = 0.5$

L = 0					
β	Real η_L	Real σ_L	Real σ'_L	Imaginary η_L	Imaginary σ_L and σ'_L
0.00	-0.2441	-0.2441	-0.2389	0.0000	0.0000
0.25	-0.2683	-0.2694	-0.2642	0.2069	0.2071
0.50	-0.3211	-0.3220	-0.3210	0.3873	0.3880
1.00	-0.4492	-0.4498	-0.4496	0.6835	0.6840
1.50	-0.5802	-0.5811	-0.5808	0.9254	0.9263
2.25	-0.7677	-0.7685	-0.7681	1.2287	1.2290
2.50	-0.8273	-0.8280	-0.8277	1.3188	1.3190
3.00	-0.9425	-0.9439	-0.9428	1.4869	1.4870
3.50	-1.0526	-1.0529	-1.0529	1.6419	1.6419
4.00	-1.1582	-1.1589	-1.1584	1.7863	1.7863
L = 1					
0.00	0.2196	0.2196	0.2200	0.0000	0.0000
0.25	0.2173	0.2172	0.2177	0.1047	0.1048
0.50	0.2106	0.2105	0.2110	0.2089	0.2090
1.00	0.1848	0.1846	0.1851	0.4130	0.4132
1.50	0.1449	0.1446	0.1451	0.6090	0.6093
2.25	0.0660	0.0656	0.0660	0.8843	0.8846
2.50	0.0361	0.0357	0.0361	0.9709	0.9712
3.00	-0.0278	-0.0278	-0.0273	1.1368	1.1370
3.50	-0.0941	-0.0946	-0.0942	1.2934	1.2936
4.00	-0.1630	-0.1635	-0.1631	1.4418	1.4419

L = 2

β	Real η_L	Real σ_L	Real σ_L'	Imaginary η_L	Imaginary σ_L and σ_L'
0.00	0.4646	0.4646	0.4646	0.0000	0.0000
0.25	0.4640	0.4639	0.4640	0.0688	0.0688
0.50	0.4622	0.4621	0.4622	0.1375	0.1375
1.00	0.4551	0.4550	0.4551	0.2745	0.2745
1.50	0.4435	0.4434	0.4435	0.4105	0.4105
2.25	0.4179	0.4178	0.4179	0.6116	0.6117
2.50	0.4074	0.4073	0.4073	0.6777	0.6778
3.00	0.3835	0.3834	0.3835	0.8083	0.8084
3.50	0.3563	0.3561	0.3562	0.9365	0.9366
4.00	0.3260	0.3258	0.3259	1.0622	1.0622

TABLE II. The exact and semiclassical phase shifts for $n = 2.0$.

L = 0					
β	Real η_L	Real σ_L	Real σ_L'	Imaginary η_L	Imaginary σ_L and σ_L'
0.00	0.1296	0.1295	0.1293	0.0000	0.0000
0.25	0.1290	0.1287	0.1285	0.0625	0.0624
0.50	0.1269	0.1267	0.1265	0.1248	0.1247
1.00	0.1188	0.1188	0.1186	0.2487	0.2487
1.50	0.1059	0.1059	0.1058	0.3709	0.3708
2.25	0.0785	0.0785	0.0785	0.5499	0.5498
2.50	0.0675	0.0675	0.0675	0.6082	0.6082
3.00	0.0432	0.0433	0.0432	0.7228	0.7228
3.50	0.0162	0.0162	0.0162	0.8345	0.8345
4.00	-0.0130	-0.0129	-0.0129	0.9433	0.9433
L = 1					
0.00	1.2368	1.2367	1.2367	0.0000	0.0000
0.25	1.2364	1.2363	1.2362	0.0542	0.0542
0.50	1.2352	1.2351	1.2351	0.1083	0.1083
1.00	1.2304	1.2304	1.2303	0.2162	0.2161
1.50	1.2226	1.2225	1.2224	0.3235	0.3234
2.25	1.2054	1.2054	1.2053	0.4825	0.4824
2.50	1.1983	1.1983	1.1982	0.5350	0.5350
3.00	1.1823	1.1823	1.1821	0.6387	0.6387
3.50	1.1639	1.1638	1.1638	0.7409	0.7409
4.00	1.1435	1.1435	1.1434	0.8415	0.8415

Table II Contd....

L = 2

β	Real η_L	Real σ_L	Real σ_L'	Imaginary η_L	Imaginary σ_L and σ_L'
0.00	2.0222	2.0221	2.0222	0.0000	0.0000
0.25	2.0220	2.0220	2.0219	0.0450	0.0449
0.50	2.0214	2.0213	2.0213	0.0900	0.0899
1.00	2.0189	2.0188	2.0187	0.1799	0.1799
1.50	2.0147	2.0146	2.0146	0.2695	0.2695
2.25	2.0055	2.0054	2.0053	0.4034	0.4034
2.50	2.0016	2.0016	2.0015	0.4478	0.4479
3.00	1.9927	1.9926	1.9926	0.5363	0.5363
3.50	1.9824	1.9824	1.9824	0.6242	0.6242
4.00	1.9706	1.9705	1.9705	0.7114	0.7114

TABLE III. The exact and semiclassical phase shifts for $n = 10.0$

L = 0					
β	Real η_L	Real σ_L	Real σ_L'	Imaginary η_L	Imaginary σ_L and σ_L'
0.00	13.8029	13.8030	13.8030	0.0000	0.0000
0.25	13.8029	13.8029	13.8029	0.0125	0.0124
0.50	13.8029	13.8028	13.8028	0.0250	0.0249
1.00	13.8028	13.8028	13.8027	0.0500	0.0500
1.50	13.8027	13.8026	13.8025	0.0750	0.0750
2.25	13.8025	13.8024	13.8023	0.1125	0.1125
2.50	13.8024	13.8024	13.8023	0.1250	0.1250
3.00	13.8022	13.8022	13.8021	0.1500	0.1500
3.50	13.8019	13.8019	13.8018	0.1750	0.1750
4.00	13.8016	13.8016	13.8015	0.1999	0.1999
L = 1					
0.00	15.2740	15.2741	15.2741	0.0000	0.0000
0.25	15.2740	15.2740	15.2740	0.0124	0.0123
0.50	15.2740	15.2739	15.2739	0.0248	0.0247
1.00	15.2740	15.2739	15.2739	0.0497	0.0496
1.50	15.2749	15.2738	15.2738	0.0745	0.0745
2.25	15.2736	15.2735	15.2735	0.1118	0.1118
2.50	15.2735	15.2735	15.2734	0.1242	0.1242
3.00	15.2733	15.2732	15.2732	0.1490	0.1490
3.50	15.2730	15.2729	15.2729	0.1738	0.1738
4.00	15.2727	15.2727	15.2727	0.1987	0.1987

Table III Contd...

L = 2

β	Real η_L	Real σ_L	Real σ_L'	Imaginary η_L	Imaginary σ_L and σ_L'
0.00	16.6474	16.6475	16.6475	0.0000	0.0000
0.25	16.6474	16.6474	16.6474	0.0123	0.0121
0.50	16.6474	16.6473	16.6473	0.0245	0.0244
1.00	16.6474	16.6474	16.6473	0.0490	0.0489
1.50	16.6473	16.6473	16.6471	0.0735	0.0735
2.25	16.6470	16.6469	16.6469	0.1103	0.1103
2.50	16.6470	16.6469	16.6468	0.1226	0.1226
3.00	16.6467	16.6467	16.6466	0.1471	0.1471
3.50	16.6465	16.6464	16.6464	0.1716	0.1716
4.00	16.6462	16.6462	16.6461	0.1961	0.1961

imaginary potential becomes stronger. The perturbative method, on the other hand, gives a real part which does not depend on the imaginary part, as is evident from Eq. (3.30).

(b) The imaginary part of the phase shift shows a monotonic increase as β increases, though not as fast as is given by the perturbative method. For small values of β , the perturbative results are close to the exact values, but deviate increasingly as β increases. Again, with an increase in L , $I_m \eta_L$ decreases. Physically this means that partial waves with higher L are less absorbed because of the centrifugal barrier.

(c) For the potential considered, the correction term of order \hbar^2 is small in the case of the first model equation. But for the second model equation this contribution is significant. This is easy to understand. In the case of the first model equation, there is a cancellation between the correction terms that does not happen in the other case. Terms of higher order in \hbar^2 depend on the higher derivatives of the function $t_1(y)$ which are anyway small for the present problem. However, one may consider a potential which changes rapidly in the vicinity of the turning point. The correction terms may be quite large in that case. For higher L , the correction terms become smaller.

(d) As is evident from the tables I - III, both model equations give almost equally good results.

(e) For fixed L and β , the phase shifts increase with the Sommerfeld parameter n . For a large n , the problem is almost the coulomb scattering problem as is evident from Table III.

III.3. Exponential and Yukawa potentials

It may be useful to apply the CMG method to some other simple cases to test the accuracy and the efficacy of the method. This motivated us to consider Exponential and Yukawa potentials:

$$(a) \text{ Exponential: } V = -V_0 e^{-\gamma r}, \quad \dots(3.32)$$

and

$$(b) \text{ Yukawa : } V = -\frac{V_0}{r} e^{-\gamma r} . \quad \dots(3.33)$$

First, we have considered the real potentials and compared our results (calculated upto \hbar^2 terms) with the exact phase shifts as well as with the results obtained with different approximation methods. The potentials are then made complex by giving V_0 a complex value ($V_0 = \mathcal{V} + i\omega$). The path integration is done along the contributing complex trajectory. The variations of the real and imaginary parts of the phase shifts with ω have also been studied. The perturbative semiclassical calculation has also been done for the sake of completeness.

III.3.1. Real potentials

The phase shifts for a real potential in the CMG method can be approximated as

$$\delta_L \approx \int_{y_t}^{\tilde{y}} \sqrt{\Upsilon(y)} \frac{dy}{y} - \sqrt{\tilde{y}^2 - (L + \frac{1}{2})^2} + (L + \frac{1}{2}) \cos^{-1} \left(\frac{L + \frac{1}{2}}{\tilde{y}} \right) + \frac{1}{12} \int_{y_t}^{\infty} \mathcal{O}[\Upsilon(y)] \sqrt{\Upsilon(y)} \frac{dy}{y} \dots(3.34)$$

where terms of order \hbar^2 have been included.

In above, y_t is the turning point and \tilde{y} is a large value of y so that $V(\frac{\tilde{y}}{K}) \ll 1$. The function $\Upsilon(y)$ is given by

$$\Upsilon(y) = y^2 - \left(\frac{y^2}{K^2}\right) V\left(\frac{y}{K}\right) - (L + \frac{1}{2})^2, \dots(3.35)$$

and

$$t_1(y) = \Upsilon(y)/y^2 \dots(3.36)$$

The $\mathcal{O}[\Upsilon(y)]$ is given by equation (2.14). In above, Langer's substitution has been made use of. The Schrödinger

equation for a field-free particle has been chosen as the model equation. The calculated phase shifts depend only weakly on the choice of the model equation. The accuracy of this simple formula (3.34) is checked by comparing the calculated phase shifts with the exact phase shifts and also the phase shifts obtained by different approximation methods. We have chosen $K = 1 \text{ fm}^{-1}$, and have shown in Table IV the different results. The exact results (A) have been taken from Wojtczak⁵. The other results are: (B) the results obtained by us, (C) the results obtained by Swan⁶ using a modified Born's approximation and (D) the approximation results of Wojtczak. It is seen that for both the Exponential and Yukawa potentials, our results are accurate even when the energy is not too high i.e., for $K \sim 1 \text{ fm}^{-1}$. The accuracy improves considerably as L increases.

It may be pointed out that the method is better suited for cases where an exactly solvable model equation is readily available. The model equation should preferably have the same analytic form as the equation being studied. In particular, the two equations should have similar behaviour near their singular points. Even when the natures of singularities are different, the phase shifts calculated by this method often come out fairly accurately, particularly if the singularity is in the inaccessible region (say at the origin). The accuracy of this method prompts one to consider a complex generalization of this method.

TABLE IV. Phase shifts for real potentials with
 $K = 1.00 \text{ fm}^{-1}$.

Potentials	L	A Exact	B Our	C Swan	D Wojtczak
$V = -V_0 e^{-\gamma r}$	0	1.0890	1.0833	0.9844	1.1588
$V_0 = 5.2283$	1	0.3931	0.3907	0.4039	0.3945
$\gamma = 1.5925$	2	0.0985	0.0952	0.1103	0.1099
$V = -V_0 \frac{1}{r} e^{-\gamma r}$	0	1.1151	1.1517	0.9685	1.2284
$V_0 = 1.5933$	1	0.3983	0.4044	0.4464	0.3822
$\gamma = 0.6279$	2	0.1627	0.1658	0.2314	0.1914

III.3.2. Scattering from Complex potentials

The expression (3.34) for phase shifts can be used even when V_0 in (3.32) and (3.33) are given complex values. However, some comments are in order. The integral on the R.H.S. is now to be taken on a complex trajectory. The details of path integration are discussed in section II.3. In the general semiclassical theory with a complex potential, there is a problem of choosing the trajectories that will make significant contributions. The problem has been studied by Knoll and Schaeffer⁷, particularly in connection with heavy ion scattering. The problem is more acute there because the Woods-Saxon optical potential leads to infinite number of complex turning points. However, Knoll and Schaeffer have given some prescriptions for locating the turning point/points which can make significant contributions. In most cases of physical interest in heavy ion scattering, only one trajectory makes a dominant contribution. At intermediate energies, there is a range of L values when 2 or 3 turning points contribute, but if the absorptive part \mathcal{Q} is large, the turning points deep inside may not again be important because of a strong absorption. The simple cases we are studying here, of course, present no such problems. The turning point which is to be considered is the analytic continuation of the real root when $\mathcal{Q} = 0$. The calculated values of some phase shifts for $K = 1.0 \text{ fm}^{-1}$ are shown in Tables V & VI.

TABLE V. Complex phase shifts for $K = 1.00 \text{ fm}^{-1}$.

$$\text{Potential: } V = -V_0 e^{-\gamma r}, \quad V_0 = \vartheta + i\omega,$$

$$\vartheta = 5.2283 \quad \text{and} \quad \gamma = 1.5925$$

ω	$\text{Re } \delta_L$	$\text{Im } \delta_L$
L = 0		
0.001	1.0394	0.0002
0.01	1.0395	0.0017
0.05	1.0396	0.0088
0.10	1.0399	0.0176
0.20	1.0407	0.0355
0.30	1.0419	0.0535
0.40	1.0435	0.0716
0.50	1.0453	0.0898
L = 1		
0.001	0.4061	0.0001
0.01	0.4062	0.0011
0.05	0.4064	0.0054
0.10	0.4070	0.0110
0.20	0.4087	0.0223
0.30	0.4110	0.0337
0.40	0.4138	0.0452
0.50	0.4168	0.0567
L = 2		
0.001	0.0916	0.0000
0.01	0.0916	0.0002
0.05	0.0915	0.0009
0.10	0.0915	0.0018
0.20	0.0914	0.0037
0.30	0.0914	0.0057
0.40	0.0913	0.0076
0.50	0.0912	0.0096

TABLE VI. Complex phase shifts for $K = 1.00 \text{ fm}^{-1}$.
 Potential: $V = -V_0 \frac{1}{r} e^{-\gamma r}$, $V_0 = \mathcal{V} + i\omega$,
 $\mathcal{V} = 1.5933$ and $\gamma = 0.6279$

ω	Re δ_L	Im δ_L
L = 0		
0.001	1.1458	0.0007
0.01	1.1459	0.0071
0.05	1.1474	0.0361
0.10	1.1510	0.0733
0.20	1.1626	0.1493
0.30	1.1787	0.2274
0.40	1.1984	0.3074
0.50	1.2209	0.3894
L = 1		
0.001	0.4057	0.0003
0.01	0.4057	0.0028
0.05	0.4056	0.0144
0.10	0.4055	0.0292
0.20	0.4040	0.0587
0.30	0.4026	0.0881
0.40	0.4006	0.1174
0.50	0.3979	0.1466
L = 2		
0.001	0.1656	0.0001
0.01	0.1656	0.0010
0.05	0.1655	0.0054
0.10	0.1655	0.0110
0.20	0.1651	0.0223
0.30	0.1648	0.0335
0.40	0.1644	0.0447
0.50	0.1639	0.0559

III.3.3. Perturbative treatment

It has been pointed out in section III.2.3., that when one uses the first order perturbative semi-classical method for complex potential, the real part of the phase shift is independent of ω while the imaginary part is proportional to ω . For complex Exponential potential, the imaginary part of the phase shifts is given by

$$I_m \delta_L = \omega/2 \int_{r_0}^{\infty} \frac{y e^{-y/Kd}}{\sqrt{y^2 + Uy^2 e^{-y/Kd} - (L + \frac{1}{2})^2}} dy$$

... (3.38)

For complex Yukawa potential one gets a similar expression:

$$I_m \delta_L = \omega/2 \int_{r_0}^{\infty} \frac{K e^{-y/Kd}}{\sqrt{y^2 + UyK e^{-y/Kd} - (L + \frac{1}{2})^2}} dy$$

...(3.39)

where r_0 is the corresponding turning point. The values of $I_m \delta_L$ obtained from (3.38) and (3.39) have been compared with the CMG values for $K = 1 \text{ fm}^{-1}$ and $L = 0$ and are shown in Fig. 3.3.

Fig. 3.3. Imaginary part of the phase shifts for a complex Yukawa potential. The parameters are as in Table VI.

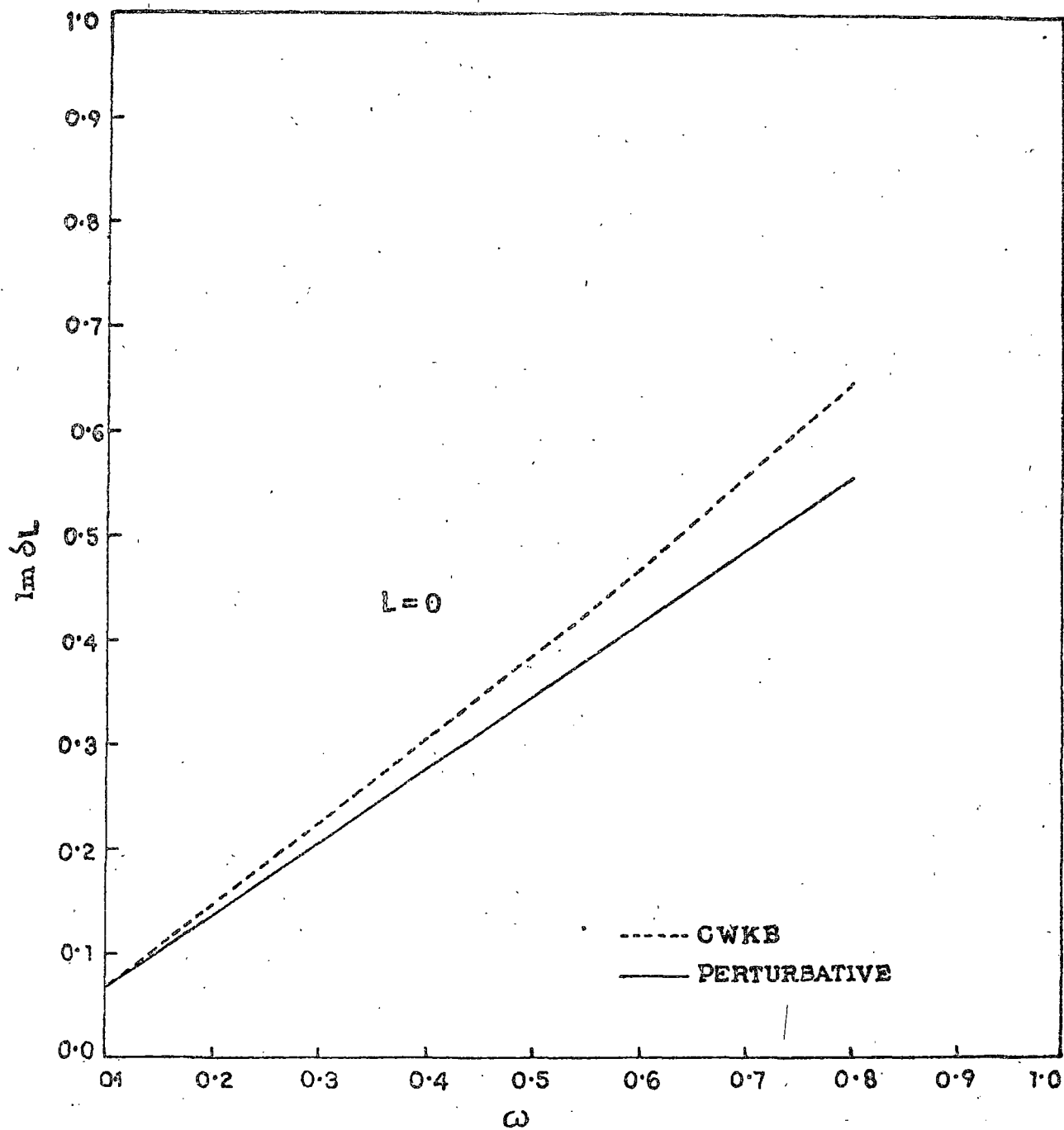


FIG. 3.3.

III.3.4. Results and conclusions

The study of the exponential and Yukawa potentials leads to the following conclusions:

1. The semiclassical results calculated by the CMG method are fairly accurate and agree well with the exact results obtained numerically.
2. The real part of the phase shifts varies slowly as ω varies. But the imaginary part shows a rapid change. If one follows a perturbative approach for the imaginary part, one naturally gets, in the first order approximation in ω , a linear relation between $I_m \delta_L$ and ω . This is a good approximation for small ω , as can be seen from Fig. 3.3 also.
3. We have considered here a case where both the real and the imaginary parts of the potential have the same radial dependence. The situation where the radial dependence is different may, in general, be more difficult, as has been pointed out by Schaeffer⁸ in connection with a complex Woods-Saxon type potential. The complication is due to the presence of an additional contribution from the sharp edge of the imaginary part of the heavy ion potential.
4. The first order quantum correction is significant here. On the average, the \hbar^2 term makes a contribution which is about 3% - 5% of the total phase shifts.

In conclusion, we have shown that the CMG method has the accuracy desirable in a semiclassical calculation for simple potential scattering. For heavy ion scattering, the potentials are, of course, more involved in the sense that more than one turning points may appear. Thus, apart from accuracy, there is also the question of the suitability of the method as a simple working technique. This is the point we would like to study in the next chapter by considering a typical heavy ion scattering experiment.

REFERENCES

1. S. Mukherjee and S.S. Chandel, J. Phys. A. 11, 1257 (1978).
2. S. S. Chandel and S. Mukherjee, J. Phys. A. 12, 329 (1979).
3. R. K. Samanta and S. Mukherjee, Phys. Rev. D26, 2916 (1982).
4. R. K. Samanta, A.K. Roy and S. Mukherjee, Proc. Nucl. and Solid State Phys. Symp. (India), 25B, 164 (1982).
5. L. Wojtczak, Nucl. Phys. 48, 325 (1963).
6. P. Swan, Nucl. Phys. 18, 245 (1960).
7. J. Knoll and R. Schaeffer, Phys. Lett. 52B, 131 (1974); Ann. Phys. (N.Y.) 97, 307 (1976); Phys. Rep. 31C, 159 (1977).
8. R. Schaeffer, Theoretical Methods in Medium energy and heavy ion Physics, eds., K.W. McVoy and W.A. Friedman (Plenum Publishing Corporation), pp. 189 - 234.